

## Unveiling the Role of lncRNA BBOX1-AS1, HOXB7, and IGF2BP1 in Non-Melanocytic Skin Tumors: Potential Biomarkers for Diagnosis

Sara A. El Derbaly<sup>1</sup>, Maha AF Hamouda<sup>1</sup>, Mohamed Abdallah Elnahas<sup>2</sup>,  
Asmaa Mahfouz Hamed<sup>1\*</sup> and Eman M Abd El Gayed<sup>1</sup>

<sup>1</sup>Department of Medical Biochemistry & Molecular Biology, <sup>2</sup> Department of Plastic Surgery,  
Faculty of Medicine, Menoufia University, Egypt

\*Corresponding author: Asmaa Mahfouz Hamed, E-mail: Asmaa.Mahfouz@med.menofia.edu.eg,  
Mobile No:01008028819

### ABSTRACT

**Background:** The primary kinds of non-melanoma malignant skin cancer (NMSC) that affect the skin were cutaneous squamous cell carcinoma (cSCC) and basal cell carcinoma (BCC). Examining new biomarkers may enhance the precision of diagnosis and therapeutic approaches.

**Objectives:** The goal of this research is to evaluate the expression of the lncRNA BBOX1-AS1, HOXB7 and IGF2BP1 and to investigate their potential use as diagnostic biomarkers in NMSC cases.

**Subjects and methods:** Thirty people participated in the current investigation. They were separated into two cohorts: Cohort I consisted of 15 tissue samples from the cSCC tumour mass (Ia) and 15 tissue samples from the same case's healthy marginal skin (Ib). Additionally, Cohort II was split into 15 tissue samples from the BCC tumour mass (IIa) and 15 tissue samples from the same case's healthy marginal skin who also had a BCC diagnosis (IIb). Their tissue lncRNA BBOX1-AS1, HOXB7 and IGF2BP1 expression levels were estimated using a quantitative real-time reverse transcriptase-polymerase chain reaction (RT-PCR) method.

**Results:** Compared to healthy marginal tissues, the malignant tissues of cSCC and BCC showed increased expression levels of the lncRNA BBOX1-AS1, HOXB7 and IGF2BP1. IGF2BP1 was found to be the most important factor linked to cSCC risk by univariate analysis, followed by BBOX1-AS1. **Conclusion:** Our findings indicated that malignant cells of cSCC and BCC have increased levels of the lncRNA BBOX1-AS1, HOXB7 and IGF2BP1. Given that BBOX1-AS1 and HOXB7 exhibited strong discriminatory power in both tumour types.

**Keywords:** cSCC, BCC, BBOX1-AS1, HOXB7, IGF2BP1, RT-PCR.

### INTRODUCTION

A global public health concern at the moment is non-melanoma skin cancer (NMSCs) <sup>(1)</sup>. Also, known as keratinocyte tumour, it encompasses cSCC and BCC <sup>(2)</sup>. According to <sup>(3)</sup>, BCC is the most prevalent kind of tumour worldwide. It accounts for 80% of keratinocyte malignancies <sup>(4)</sup>. The malignant proliferation of keratinocytes originating from the epidermis and adnexal tissues causes cSCC, the 2<sup>nd</sup> most frequent tumour in humans and approximately one-third of all NMSCs <sup>(5)</sup>. BBOX1AS1 is a 943 bp human lncRNA that was just found <sup>(6)</sup>. The chromosome 11p14.2-p14.1 contains it <sup>(7)</sup>. BBOX1-AS1 contributes to the formation of tumours in an oncogenic manner. Increased cell aggressiveness and metastasis are all consequences of BBOX1-AS1 overexpression. Furthermore, BBOX1-AS1 inhibits tumour cell death and increases its survival. It is associated with poor prognostic variables and unfavourable clinicopathological aspects, including as disease-free survival, overall survival, tumour size, clinical stage, and lymph node metastases. These results highlight the importance of BBOX1-AS1 as a crucial regulator in a number of tumour metastasis-related processes <sup>(8)</sup>.

It has been established that BBOX1-AS1 has a role in controlling the Hedgehog signalling pathway and other tumour-related signalling pathways <sup>(9)</sup>. By upregulating Homeobox B7 (HOXB7) expression, BBOX1-AS1 stimulates the Wnt/ $\beta$ -catenin pathway, boosting tumour progression and MELK/FAK signaling through improving the malignant behaviour of cells, comprising cell migration, invasion, and proliferation

<sup>(10)</sup>. One class I homeobox member that is crucial to carcinogenesis is HOXB7. However, other researchers found that HOXB7 promotes the development of multipotent mesenchymal cells and haematopoietic stem cells <sup>(11)</sup>. Many growth tumour factors were all up-regulated by HOXB7 contributing to angiogenesis <sup>(12)</sup>. In head and neck SCC, there was a substantial overexpression of the HOXB7 protein and mRNA, this overexpression is strongly linked to poor prognosis <sup>(11)</sup>.

Six RNA binding domains of the RNA-binding protein insulin growth factor2 binding protein 1 regulate the translation, localisation, stability, and alternative splicing of its target mRNA. Additionally, cases with a variety of tumours have a bad prognosis when their IGF2BP1 expression is high <sup>(13)</sup>.

### SUBJECT AND METHODS

**Subjects:** The Departments of Plastic Surgery and Medical Biochemistry & Molecular Biology, Faculty of Medicine, Menoufia University collaborated to conduct this research. From June 2023 to March 2024, 30 participants with histological evidence of non-melanoma skin tumour (BCC or SCC) were chosen from the Menoufia University Hospital's Plastic Surgery Department. They were divided into the subsequent cohorts: Cohort I consisted of 15 tissue samples from the SCC tumour mass (Ia) and 15 tissue samples from the same case's healthy marginal skin (Ib). Cohort II consisted of 15 tissue samples from the BCC tumour mass (IIa) and 15 tissue samples from the same case's healthy marginal skin (IIb).

A thorough examination of each participant began with a review of their medical history, which included information on their name, age, sex, occupation and history of the disease (including the origin, progression, and duration of tumour, as well as any drug use). In order to rule out systemic disorders, a thorough general examination was conducted. A preoperative incisional biopsy was used to do a histological study in order to confirm the diagnosis. In cases of cSCC, neck ultrasonography was used to examine lymph node metastases.

**Tissue sampling:** Each case had three biopsies obtained: The first was used for histological analysis until a diagnosis was made. The second and third were then taken in two Eppendorf tubes, one from a skin lesion that was pathologically determined to be non-melanocytic skin tumour and the other from the case's healthy marginal skin. They were then frozen at -80 degrees Celsius for further RNA extraction.

**Histopathological evaluation:** Each case's Haematoxylin and eosin- stained slides were examined to verify the diagnosis and evaluate the following: Regional lymph node and pathologic stage for cSCC were evaluated, together with histologic type, grade, tumour infiltrating lymphocyte, lymph vascular invasion, and perineural invasion.

**RNA extraction:** Regarding the manufacturer's instructions, the Qiagen™ RNA tissue RNeasy Mini Kit (Cat. No. 217004) was used to extract the mRNA molecules from tissue in a pure manner.

**First-Step PCR (RT-PCR):** Applied Biosystems, USA, 2012, High-Capacity cDNA Reverse Transcription Kits (Cat. No. 4374966) were used to create the complementary DNA. The following circumstances were present when cDNA synthesis was carried out: Two microlitres of 10x RT buffer, 0.8 microlitres of 25x dNTP mix, 1 microlitre of 10x MultiScribe Reverse Transcriptase mix, 2 microlitres of RT primers, 10 microlitres of extracted RNA, 1 microlitre of RNase Inhibitor, and 3.2 microlitres of RNase-free water made up the final volume of 20 microlitres. After 10 minutes of annealing at 25°C, the reverse transcription process took place for 120 minutes

at thirty-seven degrees Celsius. After that, enzyme inactivation was done for five minutes at 85°C. Up until the real-time PCR, the resultant cDNA was kept at -20°C.

**Second step (Real-Time PCR):** Thermo Scientific Maxima SYBR Green, ROX Master Mix 2X (Cat. No. K0221) was used for the procedure. The primers used for the housekeeping genes GAPDH, IGF2BP1, HOXB7, and LncRNA BBOX1-AS1 were illustrated in table (1).

**Table (1):** Gene specific primers utilized in PCR

	Forward primer	Reverse primer
<b>BBOX1-AS1</b>	5'-GATGGGCACA TTTGAAGTT-3'	5'-CAGCGTTAGG TTTGGAGTTG-3'
<b>HOXB7</b>	5'-TTCCCAGAAC AAACTTCTTGTGC	5'-GCATGTTGAA GGAAGCTCGGCT-3'
<b>IGF2BP</b>	5'- GCGGCCAGTTC TTGGTCAA-3'	5'- TTGGGCACCG AATGTTCAATC-3'
<b>GAPDH</b>	5'-CCACTCCTCCA CCTTTGAC-3'	5'-ACCCTGTTGC TGTAGCCA-3'

The following parameters were used for the runs: 12.5 microliters of Maxima SYBR Green qPCR Master Mix, 1 microliter of Template cDNA, 1 µl for each of the gene's forward and reverse primers, and 9.5 microliters of RNase-free water made up the total volume of 25 microliters. After 10 minutes of initial activation at 95°C, there were forty cycles of denaturation at 95°C for fifteen seconds, annealing, and extension at 60°C for 60 seconds. Version 2.0.1 of the Applied Biosystems 7500 software has been applied to analyses the data. The comparative  $\Delta\Delta$  Ct technique has been applied to carry out the relative quantification (RQ) of gene expression <sup>(14)</sup>.

The expression level of the housekeeping gene GAPDH has been used to normalise the levels of the lncRNAs BBOX1-AS1, HOXB7, and IGF2BP1. Each run was concluded with a melting curve analysis to confirm primer dimer absence and amplification specificity. 95°C for fifteen seconds, 55°C for one minute of fluorescence data collecting, 95°C for thirty seconds, and 55°C for 15 s comprised the melting curve cycling program. Melting curves and an amplification plot were produced (**Figure 1: a, b, c & d**).

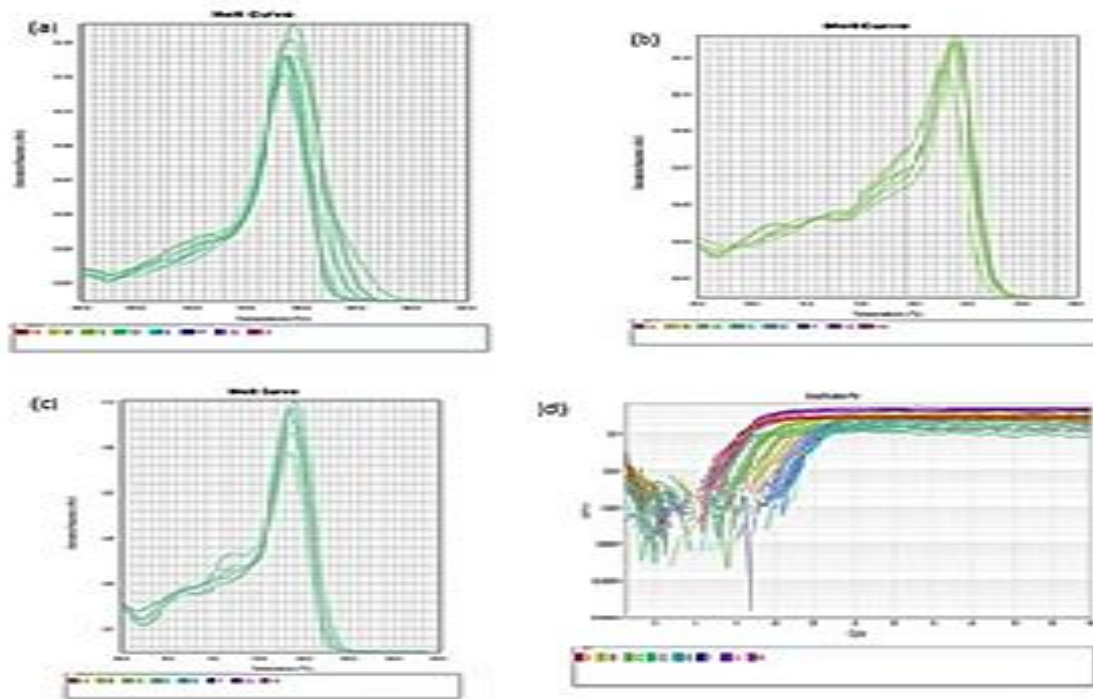


**Fig (1): Melting curves of BBOX1-AS1 (a), HOXB7 (b), IGF2BP1 (c) and an amplification plot (d).**

**Ethics declarations:** Every participant in the study signed a written consent form. The research protocol was approved by the Menoufia University Faculty of Medicine's Committee of Medical Research Ethics under code 4/2023 BIO 35. The Helsinki Declaration's guidelines were followed in the research.

#### Statistical Analysis

Epi Info 2000 and SPSS version 20 were used to analyze the data. Frequency and percentage have been utilized to display qualitative data. Standard deviation (SD), mean, range, and median have been utilized to communicate quantitative data. Among the statistical studies were the Chi-square test or Fisher exact test for evaluating correlations between qualitative variables and the student's t-test for comparing two cohorts with quantitative data that was normally distributed. The Kruskal-Wallis test for multiple cohort comparisons, the Mann-Whitney U test for comparing two

independent cohorts, and the Wilcoxon signed-rank test for comparing two dependent cohorts in quantitative variables with abnormal distributions were examples of non-parametric tests.

Relationships between quantitative variables that were not regularly distributed were assessed using Spearman correlation. The biomarkers' sensitivity, specificity, positive predictive value, and negative predictive value were ascertained by ROC curve analysis. The primary factors associated with NMSC were determined using logistic regression analysis. Statistical significance has been established at a p-value  $\leq 0.05$ .

#### RESULTS

Regarding sex, age, smoking, sun exposure, and other comorbidities, there were a statistically insignificant variances among the two cohorts under study (Table 2).

**Table (2):** Demographic and clinical data of the studied cohorts

	Cohort I (n = 15)		Cohort II (n = 15)		Test of Sig.	p
	No.	%	No.	%		
<b>Gender</b>						
Male	11	73.3	13	86.7	$\chi^2= 0.833$	<sup>FE</sup> p=0.651
Female	4	26.7	2	13.3		
<b>Age (years)</b>						
Min. – Max.	25.0 – 80.0		37.0 – 75.0		t=0.108	0.915
Mean ± SD.	63.60 ± 13.36		63.13 ± 10.15			
Median (IQR)	66.0(61.0 – 71.50)		63.0 (59.0 – 71.0)			
<b>Sun exposure</b>	12	80.0	13	86.7	$\chi^2= 0.240$	<sup>FE</sup> p=1.000
<b>Family history</b>	0	0.0	0	0.0	$\chi^2= -$	–
<b>Smoking</b>	2	13.3	2	13.3	$\chi^2= 0.000$	1.000
<b>Comorbidities</b>	9	60.0	9	60.0	$\chi^2= 0.000$	1.000
HTN	7	46.7	8	53.3	$\chi^2= 0.133$	0.715
Virus C	4	26.7	2	13.3	$\chi^2= 0.833$	<sup>FE</sup> p=0.651
DM	6	40.0	0	0.0	$\chi^2= 7.500^*$	<sup>FE</sup> p=0.017*

There were no appreciable variations between the cohorts in terms of TILs, LVI, colour, consistency, or the quantity of lesions (Table 3).

**Table (3):** Statistical comparison between the two studied cohorts according to tumour criteria

	Cohort Ia (n = 15)		Cohort IIa (n = 15)		Test of sig.	p
	No.	%	No.	%		
<b>Number of lesions</b>						
Single	9	60.0	13	86.7	FET= 3.774	0.394
Two	3	20.0	2	13.3		
Three	1	6.7	0	0.0		
Four	1	6.7	0	0.0		
Multiple	1	6.7	0	0.0		
<b>Color</b>						
Greyish white	10	66.7	8	53.3	FET= 4.274	0.195
Gray	5	33.3	3	20.0		
Brown	0	0.0	3	20.0		
Black	0	0.0	1	6.7		
<b>Consistency</b>						
Firm	7	46.7	2	13.3	$\chi^2 = 4.203$	0.157
Soft	6	40.0	11	73.3		
Rubbery	2	13.3	2	13.3		
<b>TILs</b>	0	0.0	2	13.3	$\chi^2 = 2.143$	<sup>FE</sup> p=0.483
<b>LVI</b>	1	6.7	0	0.0	$\chi^2 = 1.034$	<sup>FE</sup> p=1.000
<b>Increase N/C</b>						
No	10	66.7	10	66.7	$\chi^2 = 0.000$	1.000
Yes	5	33.3	5	33.3		

Sixty percent of cSCC cases were grade II, and twenty percent were grade I and grade III. 53.3% of cases were in stage I, 33.3% were in stage II, and 13.3% were in stage III. 86.7% of cases had nodal involvement and 6.7% had nodal involvement. Every case was M0. Additionally, 20% of cases had a positive neck ultrasound, whereas 80% of cases had a free neck ultrasound (Table 4).

**Table (4):** Distribution of the studied cases in cohort Ia according to pathological criteria (n = 15)

	No.	%
<b>Grade</b>		
I	3	20.0
II	9	60.0
III	3	20.0
<b>T stage</b>		
T1	8	53.3
T2	5	33.3
T3	2	13.3
<b>N stage</b>		
N0	13	86.7
N1	1	6.7
N2	1	6.7
<b>M stage (M0)</b>	15	100.0
<b>Neck US</b>		
Free	12	80.0
Positive LN	3	20.0

The levels of BBOX1-AS1, HOXB7, and IGF2BP1 gene expression were significantly higher in cohort Ia than in cohort Ib. In a similar vein, cohort IIa has significantly greater statistical levels of BBOX1-AS1, HOXB7, and IGF2BP1 expression than in cohort IIb. Furthermore, cohort Ia's expression levels of BBOX1-AS1, HOXB7, and IGF2BP1 were significantly greater than cohort IIa's (Table 5 and figure 2).

**Table (5):** Statistical comparison between the two studied cohorts according to BBOX1-AS1, HOXB7 and IGF2BP1 expression

		cSCC (n = 15)	BCC (n = 15)	U	p
<b>BBOX1-AS1</b>	<b>Tumour</b>				
	Min. – Max.	0.19 – 3.84	0.39 – 3.51		
	Mean ± SD.	2.76 ± 1.31	0.95 ± 0.87	38.0*	0.001*
	Median (IQR)	3.56(2.06 – 3.74)	0.70(0.43 – 0.91)		
<b>Control</b>	Min. – Max.	0.04 – 1.0	0.05 – 1.45		
	Mean ± SD.	0.50 ± 0.36	0.72 ± 0.42	91.0	0.389
	Median (IQR)	0.51 (0.15 – 0.82)	0.91 (0.43 – 0.96)		
	<b>Z(pi)</b>	3.408*(0.001*)	2.215*(0.027*)		
<b>HOXB7</b>	<b>Tumour</b>				
	Min. – Max.	0.20 – 6.66	0.42 – 4.66		
	Mean ± SD.	3.12 ± 2.13	1.66 ± 1.43	62.0*	0.037*
	Median (IQR)	2.95 (1.09 – 4.97)	0.92 (0.74 – 2.44)		
<b>Control</b>	Min. – Max.	0.15 – 1.08	0.23 – 1.94		
	Mean ± SD.	0.61 ± 0.29	0.86 ± 0.49	79.0	0.174
	Median (IQR)	0.53 (0.42 – 0.86)	0.94 (0.46 – 1.06)		
	<b>Z(pi)</b>	3.124*(0.002*)	2.442*(0.015*)		
<b>IGF2BP1</b>	<b>Tumour</b>				
	Min. – Max.	0.57 – 5.70	0.44 – 3.70		
	Mean ± SD.	2.59 ± 1.87	1.15 ± 1.10	61.0*	0.033*
	Median (IQR)	2.24 (1.02 – 4.47)	0.64 (0.56 – 0.85)		
<b>Control</b>	Min. – Max.	0.01 – 0.89	0.02 – 1.36		
	Mean ± SD.	0.43 ± 0.24	0.58 ± 0.47	76.0	0.137
	Median (IQR)	0.45 (0.26 – 0.59)	0.54 (0.13 – 1.01)		
	<b>Z(pi)</b>	3.408*(0.001*)	2.215*(0.027*)		

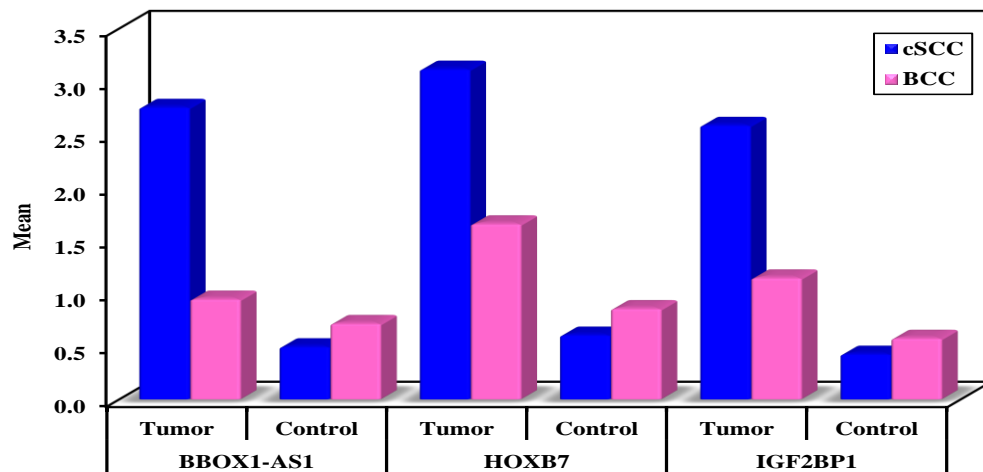


**Fig (2):** Comparison between the two studied cohorts according to BBOX1-AS1, HOXB7 and IGF2BP1

Furthermore, cohort Ia cases with high tumour grade showed considerably higher levels of IGF2BP1 expression, with grade III showed the highest expression (**Figure 3**).

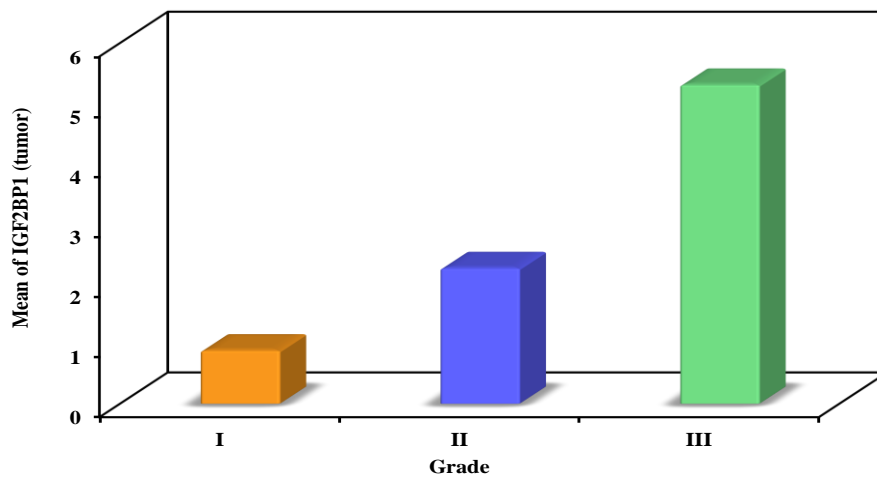


**Fig (3):** Relation between IGF2BP1 (tumour) and grade in cohort Ia

In cohort Ia, BBOX1-AS1 expression levels also markedly rose as tumour grades progressed, with grade III showed the highest expression. Additionally, there was a statistically significant association among the number of lesions in cohort Ia and BBOX1-AS1 expression, (**Figure 4**).

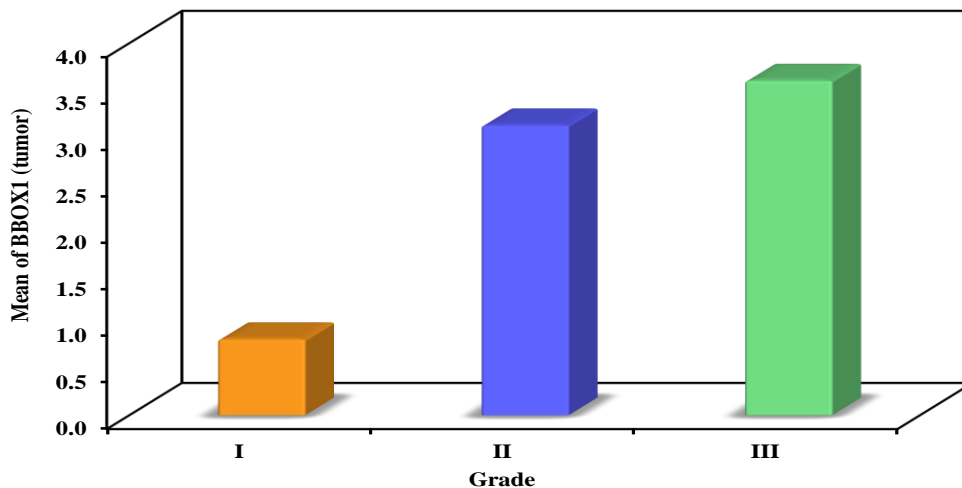


**Fig (4):** Relation between BBOX1-AS1 (tumour) and grade in cohort Ia

In terms of diagnostic performance, the sensitivity, specificity, positive predictive value, and negative predictive value for diagnosing cSCC were 86.67%, 80%, 81.2%, and 85.7% respectively at a cutoff threshold for IGF2BP1 > 0.65. These values were 80%, 73.33%, 75%, and 78.6% for HOXB7 at cutoff of > 0.826). Sensitivity, specificity, positive predictive value, and negative predictive value for expecting cSCC for BBOX1-AS1 (>0.832) were 86.67%, 80%, 81.2%, and 85.7% respectively (Figure 5).

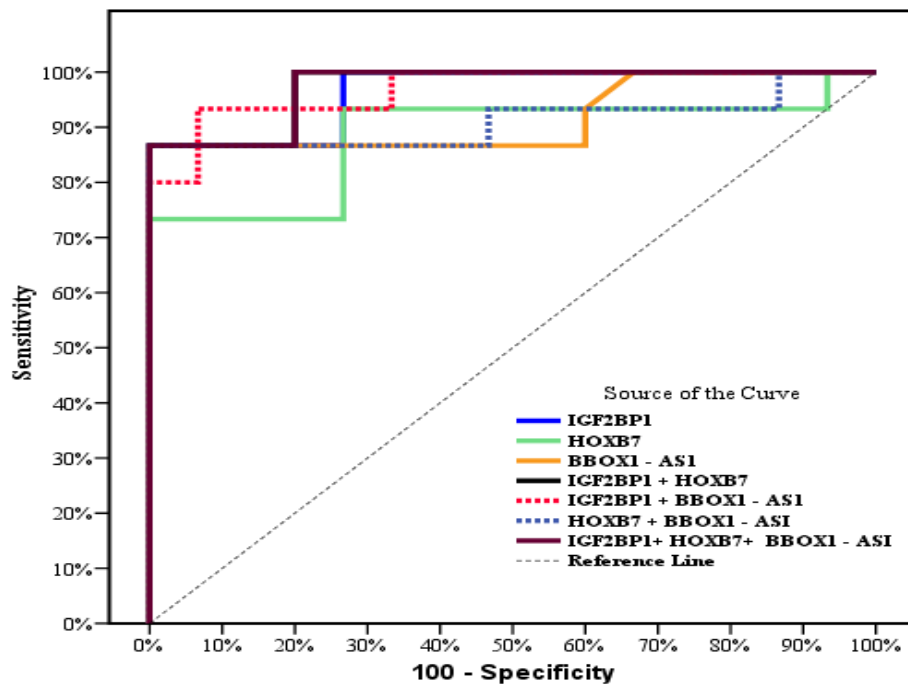


**Fig (5):** ROC curve for IGF2BP1, HOXB7 and BBOX1 to discriminate cohort Ia from cohort Ib.

These values were 66.67%, 60%, 62.5%, and 64.3% in BCC at a cutoff point for IGF2BP1 > 0.59, 60%, 46.6%, 52.9%, and 53.8% in HOXB7 at cutoff of > 0.825, and 53.33%, 53.33%, 53.3%, and 53.3% in BBOX1-AS1 at cutoff of  $\leq 0.7$  (Figure 6).

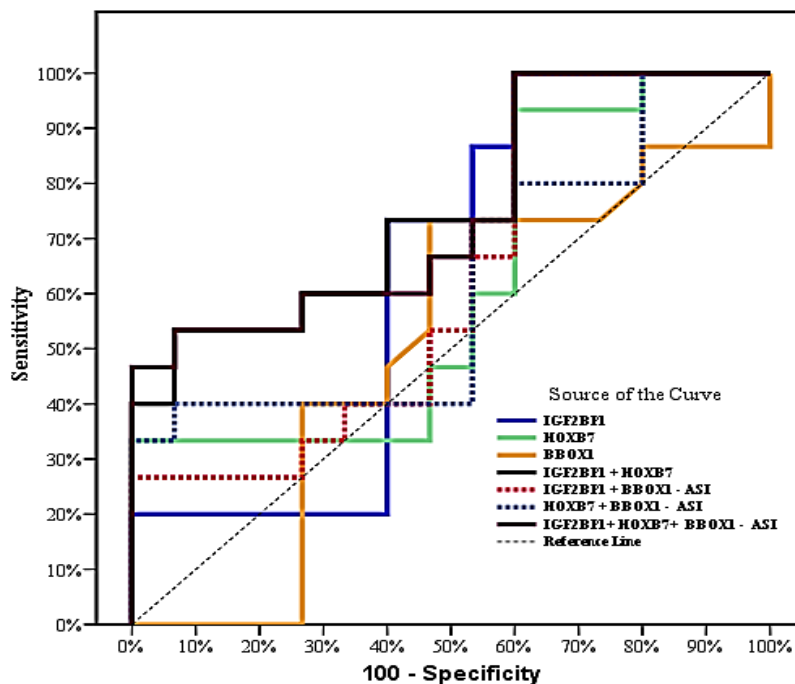


**Fig (6):** ROC curve for IGF2BP1, HOXB7 and BBOX1-AS1 to discriminate cohort IIa from cohort IIb.

The sensitivity, specificity, positive predictive value, and negative predictive value were 86.67%, 80%, 81.2%, and 85.7%, respectively, to distinguish cSCC from BCC at a cutoff point for IGF2BP1  $\geq 0.95$ . The corresponding values for HOXB7 ( $\geq 0.989$ ) were 73.33%, 66.67%, 68.7%, and 71.4%. The sensitivity, specificity, positive predictive value, and negative predictive value for BBOX1-AS1 ( $\geq 0.969$ ) were 86.67%, 80%, 81.2%, and 85.7%, in that order (Figure 7).

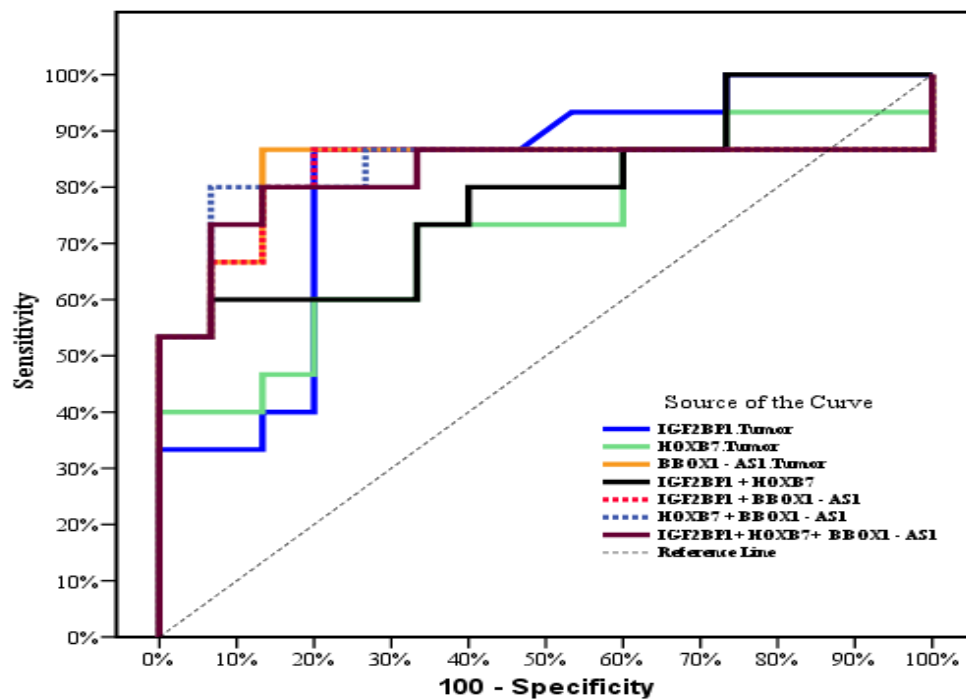


**Fig (7):** ROC curve for IGF2BP1, HOXB7 and BBOX1-AS1 to discriminate cohort Ia (n = 15) from cohort IIa (n = 15) IGF2BP1 was the parameter most substantially linked to the risk of cSCC, according to univariate analysis (OR = 2948.448, 95% CI: 5.16–1686209.49), followed by BBOX1-AS1 (OR = 8.833, 95% CI: 1.557–50.672) (Table 6).

**Table (6):** Univariate and multivariate logistic regression analysis for the parameters affecting cohort Ia (n = 15)

	Univariate		#Multivariate	
	p	OR (LL – UL 95% C.I)	p	OR (LL – UL 95% C.I)
<b>IGF2BP1</b>	<b>0.014*</b>	2948.448(5.16 – 1686209.49)	0.074	551.819(0.547 – 556775.5)
<b>HOXB7</b>	<b>0.057</b>	14.791(0.921 – 237.522)		
<b>BBOX1-AS1</b>	<b>0.014*</b>	8.833(1.557 – 50.672)	0.423	3.123(0.193 – 50.481)

## DISCUSSION

The most prevalent malignancy in the Caucasian population is NMSC, which includes actinic keratosis (AK), BCC, and SCC<sup>(15)</sup>. According to **Saizan et al.**<sup>(16)</sup>, BCC is the second most frequent skin tumour among African Americans and the most common among Caucasians, Asians, and Hispanics. However, after BCC, cSCC is the second most prevalent NMSC<sup>(17)</sup>. The cohorts in this study were matched in terms of both gender and age. Additionally, there was a statistically insignificant variance between them in terms of smoking, sun exposure, or other comorbidities. In terms of age, sex, and sun exposure,<sup>(18)</sup> there was a statistically insignificant variance between BCC and cSCC. Accordingly,<sup>(19)</sup> it was reported that no gender-specific annual differences are statistically significant. Additionally, according to **Moser et al.**<sup>(20)</sup>, the American Tumour Society has reported that NMSC has an equal sex distribution.

According to the current study, 60% of instances with cSCC had grade II, with 20% had grades I and III. Additionally, 86.7% of instances had N0, 6.7% had N1 and N2, 100% had M0, 53.3% had stage I, 33.3% had stage II, and 13.3% had stage III.

Additionally, 20% of cases had positive neck US, whereas 80% of cases had free neck US. According to **Venables et al.**<sup>(21)</sup>, using the American Joint Committee on Tumour 8 staging system, 69.9% of cases had T1 at presentation, 10.6% had T2, 19.4% had T3, and 0.1% had T4 without metastases.

According to our findings, when compared to the same case's healthy marginal skin, the tumour mass's BBOX1-AS1, HOXB7, and IGF2BP1 gene expression levels were significantly higher statistically. BBOX1-AS1 expression was found to be significantly upregulated in oral and lung SCC by **Zhao et al.**<sup>(22)</sup> and **Zhang et al.**<sup>(7)</sup>. According to **Tao et al.**<sup>(23)</sup>, hepatocellular tumour exhibits significant levels of BBOX1-AS1 expression. Additionally, **Wang et al.**<sup>(24)</sup> reported that BBOX1-AS1 is significantly expressed in colorectal tumour and that it uses competing endogenous RNA to promote the development of gastric, cervical, ovarian, and CRC tumours. BBOX1-AS1 expression rises in pituitary adenoma tissues<sup>(25)</sup>. Consequently, **Pan et al.**<sup>(26)</sup> found that the tissue of esophageal squamous cell carcinoma (ESCC) had increased levels of BBOX1-AS1 expression. According to **Sheng et al.**<sup>(10)</sup>, BBOX1-AS1 upregulates HOXB7



expression, which stimulates the Wnt/ $\beta$ -catenin pathway and enhances the malignant behaviour of ESCC cells, including invasion, migration, and proliferation, thus accelerating tumour growth. Through the Wnt signalling pathway, HOXB7 mRNA is markedly overexpressed in head and neck SCC, according to **Wu *et al.*** <sup>(11)</sup> and **Gao and Chen** <sup>(27)</sup>. According to **Samarelli *et al.*** <sup>(28)</sup>, cases with idiopathic pulmonary fibrosis (IPF) had considerable expression of HOXB7 in their lung parenchyma. High HOXB7 protein expression has been linked to a bad prognosis for individuals with malignancies of the digestive system, according to **Liu *et al.*** <sup>(29)</sup>. Additionally, **Dai *et al.*** <sup>(30)</sup> found that intrahepatic cholangiocarcinoma cell lines exhibit significant levels of HOXB7 expression. According to **Zhou *et al.*** <sup>(31)</sup>, HOXB7 is significantly expressed at both the mRNA and protein levels in glioblastoma and isocitrate dehydrogenase 1 wild type gliomas suggesting that HOXB7 is an oncogene in gliomas.

**Zhang *et al.*** <sup>(32)</sup> and **Wang *et al.*** <sup>(33)</sup> showed that esophageal SCC is associated with IGF2BP1 overexpression. Additionally, **Kim *et al.*** <sup>(34)</sup> noted that, in comparison with their corresponding controls, SCC exhibits a substantial overexpression of IGF2BP1 mRNA. Additionally, poor cell differentiation and greater SCC staging are positively connected with IGF2BP1 mRNA expression levels.

In contrast to our findings, **Lotfi *et al.*** <sup>(35)</sup> reported that lncRNAs BBOX1-AS1 and LINC00698 are higher in healthy individuals than in cases with colorectal tumour. Additionally, **Zhou *et al.*** <sup>(31)</sup> reported that 1p/19q codeletion gliomas exhibit considerable regulation of HOXB7 mRNA and protein levels. According to them, oligodendroglioma may have a point mutation or deletion of HOXB7, which lowers the mRNA level. Alternatively, post-translational modification may be the reason of the loss of protein expression. In lung tumour, **Pan *et al.*** <sup>(26)</sup> discovered that Krueppel-like factor 5 (KLF5) activates the focal adhesion kinase (FAK) signalling axis by targeting miR-27a-5p and inducing BBOX1-AS1 expression, which controls cell invasion and proliferation.

IGF2BP1 was the most significant parameter linked with the hazard of cSCC (OR, 2948.448 95% C.I (5.16–1686209.49)), followed by BBOX1-AS1 (OR, 8.833 95% C.I (1.557 – 50.672)), according to the univariate analysis of the parameters impacting cSCC. According to the multivariate study of the parameters influencing cSCC, BBOX1-AS1 and IGF2BP1 are independent risk factors. Using univariate regression models on a number of characteristics, **Kim *et al.*** <sup>(34)</sup> discovered that in cSCC, poorly differentiated cells express more IGF2BP1 mRNA than do moderately and well-differentiated cells.

A comparatively small sample size is one of the study's shortcomings that could affect how broadly the results can be applied. Inability to measure case blood expression levels and correlate them with tissue

expression at the same time. In order to confirm the diagnostic and prognostic potential of BBOX1-AS1, HOXB7, and IGF2BP1 in cSCC and BCC, bigger samples' sizes will be needed for future tissue and blood research. To evaluate their impact on the course of the disease and case outcomes, long-term monitoring is required.

## CONCLUSION

In comparison with healthy marginal skin, the study showed that the expression of BBOX1-AS1, HOXB7, and IGF2BP1 genes was significantly upregulated in cSCC and BCC tumour tissues, but with cSCC showed significantly higher expression. These biomarkers may play a part in the development of tumour, as evidenced by their correlation with tumour grade and lesion count.

**Consent for publication:** I certify that each author has granted permission for the work to be submitted.

**Funding:** No fund

**Availability of data and material:** Available

**Conflicts of interest:** None

**Competing interests:** None

## REFERENCES

1. **Thomas S, Lefevre J, Baxter G, Hamilton N (2021):** Interpretable deep learning systems for multi-class segmentation and classification of non-melanoma skin tumour. *Medical Image Analysis*, 68: 101915. <https://doi.org/10.1016/j.media.2020.101915>.
2. **Hernandez L, Mohsin N, Levin N *et al.* (2022):** Basal cell carcinoma: An updated review of pathogenesis and treatment options. *Dermatologic therapy*, 35 (6): e15501. <https://doi.org/10.1111/dth.15501>
3. **Heath M, Bar A (2023):** Basal Cell Carcinoma. *Dermatologic clinics*, 41 (1): 13–21.
4. **El-Khalawany M, Hassab-El-Naby H, Mousa A *et al.* (2022):** Epidemiological and clinicopathological analysis of basal cell carcinoma in Egyptian population: a 5-year retrospective multicenter study. *Journal of tumour research and clinical oncology*. <https://doi.org/10.1007/s00432-022-04207-7>.
5. **Chang M, Azin M, Demehri S (2022):** Cutaneous Squamous Cell Carcinoma: The Frontier of Cancer Immunoprevention. *Annu Rev Pathol.*, 17: 101-119. doi: 10.1146/annurev-pathol-042320-120056.
6. **Ma R, Lu Y, He X, Zeng X (2023):** LncRNABBOX1-AS1 targets miR-361-3p/COL1A1 axis to drive the progression of oesophageal carcinoma. *European Journal of Clinical Investigation*, 53 (4): e13929. <https://doi.org/10.1111/eci.13929>
7. **Zhang Y, Wang X, Cheng X *et al.* (2022):** Clinical significance and effect of lncRNA BBOX1-AS1 on the proliferation and migration of lung squamous cell carcinoma. *Oncology letters*, 23 (1): 17. <https://doi.org/10.3892/ol.2021.13135>.
8. **Huang Y, Hong W, Wei X (2022):** The molecular mechanisms and therapeutic strategies of EMT in tumour progression and metastasis. *Journal of hematology & oncology*, 15 (1): 129. <https://doi.org/10.1186/s13045-022-01347-8>.

9. Shi J, Yang C, An J *et al.* (2021): KLF5-induced BBOX1-AS1 contributes to cell malignant phenotypes in non-small cell lung tumour via sponging miR-27a-5p to up-regulate MELK and activate FAK signaling pathway. *Journal of experimental & clinical tumour research*. CR., 40 (1): 148. <https://doi.org/10.1186/s13046-021-01943-5>
10. Sheng J, Zhou M, Wang C *et al.* (2022): Long non-coding RNA BBOX1-AS1 exacerbates esophageal squamous cell carcinoma development by regulating HOXB7/ $\beta$ -catenin axis. *Experimental cell research*, 415 (1): 113117. <https://doi.org/10.1016/j.yexcr.2022.113117>
11. Wu X, Li J, Yan T *et al.* (2021): HOXB7 acts as an oncogenic biomarker in head and neck squamous cell carcinoma. *Cancer cell international*, 21 (1): 393. <https://doi.org/10.1186/s12935-021-02093-6>
12. Zhou T, Feng Z, Yang F *et al.* (2022): High expression of HOXB7 is an unfavorable prognostic factor for solid malignancies: A meta-analysis. *Medicine (Baltimore)*, 101 (3): e28564. <https://doi.org/10.1097/MD.00000000000028564>
13. Singh A, Singh V, Wallis N *et al.* (2024): Development of a specific and potent IGF2BP1 inhibitor: A promising therapeutic agent for IGF2BP1-expressing tumours. *European Journal of Medicinal Chemistry*, 263: 115940. <https://doi.org/10.1016/j.ejmech.2023.115940>
14. Schmittgen T, Livak K (2008): Analyzing real-time PCR data by the comparative CT method. *Nat. Protoc.*, 3 (6): 1101-1108.
15. Hyeraci M, Papanikolaou E, Grimaldi M *et al.* (2023): Systemic Photoprotection in Melanoma and Non-Melanoma Skin Tumour. *Biomolecules*, 13 (7): 1067. <https://doi.org/10.3390/biom13071067>
16. Saizan A, Taylor S, Elbuluk N (2023): Pigmented Basal Cell Carcinoma: An Argument for Sub-Classification. *Journal of drugs in dermatology*. JDD., 22 (2): 217–218.
17. Jones O, Ranmuthu C, Hall P *et al.* (2020): Recognising Skin Tumour in Primary Care. *Advances in therapy*, 37 (1): 603–616.
18. Nada H, El-Nabarawy E, Mahmoud S *et al.* (2020): Expression of microRNA-31 and microRNA-205 in basal cell carcinoma, squamous cell carcinoma, and healthy controls: a comparative study. *Journal of the Egyptian Women's Dermatologic Society*, 17 (1): 38–44.
19. Ciężkańska M, Kamińska-Winciorek G, Lange D *et al.* (2021): The incidence and clinical analysis of non-melanoma skin tumour. *Scientific reports*, 11 (1): 4337. <https://doi.org/10.1038/s41598-021-83502-8>
20. Moser U, Andrianakis A, Pondorfer P *et al.* (2020): Sex-specific differences in cases with nonmelanoma skin tumour of the pinna. *Head & neck*, 42 (9): 2414–2420.
21. Venables Z, Tokez S, Hollestein L *et al.* (2022): Validation of four cutaneous squamous cell carcinoma staging systems using nationwide data. *The British journal of dermatology*, 186 (5): 835–842.
22. Zhao C, Shi W, Chen M (2022): Long non-coding RNA BBOX1-antisense RNA 1 enhances cell proliferation and migration and suppresses apoptosis in oral squamous cell carcinoma via the miR-3940-3p/laminin subunit gamma 2 axis. *Bioengineered*, 13 (4): 11138–11153.
23. Tao H, Zhang Y, Li J *et al.* (2022): Oncogenic lncRNA BBOX1-AS1 promotes PHF8-mediated autophagy and elicits sorafenib resistance in hepatocellular carcinoma. *Molecular therapy oncolytics*, 28: 88–103. <https://doi.org/10.1016/j.omto.2022.12.005>
24. Wang Q, Li X F, Zhou Y *et al.* (2023): Long noncoding RNA BBOX1-AS1 increased radiotherapy sensitivity in colorectal tumour by stabilizing and activating PFK1. *Translational oncology*, 36: 101751. <https://doi.org/10.1016/j.tranon.2023.101751>
25. Wu H, Zhou S, Zheng Y *et al.* (2022): LncRNA BBOX1-AS1 promotes pituitary adenoma progression via sponging miR-361-3p/E2F1 axis. *Anti-tumour drugs*, 33 (7): 652–662.
26. Pan C, Chen G, Zhao X *et al.* (2022): lncRNA BBOX1-AS1 silencing inhibits esophageal squamous cell tumour progression by promoting ferroptosis via miR-513a-3p/SLC7A11 axis. *European journal of pharmacology*, 934: 175317. <https://doi.org/10.1016/j.ejphar.2022.175317>
27. Gao D, Chen H (2018): Specific knockdown of HOXB7 inhibits cutaneous squamous cell carcinoma cell migration and invasion while inducing apoptosis via the Wnt/ $\beta$ -catenin signaling pathway. *American journal of physiology. Cell physiology*, 315 (5): C675–C686. <https://doi.org/10.1152/ajpcell.00291.2017>
28. Samarelli A, Tonelli R, Raineri G *et al.* (2024): Expression of HOXB7 in the Lung of Cases with Idiopathic Pulmonary Fibrosis: A Proof-of-Concept Study. *Biomedicines*, 12 (6): 1321. <https://doi.org/10.3390/biomedicines12061321>
29. Liu F, Chen H, Xiong Y, Zhu Z (2019): Deregulated HOXB7 expression predicts poor prognosis of cases with malignancies of digestive system. *Minerva chirurgica*, 74 (5): 422–430.
30. Dai L, Hu W, Yang Z *et al.* (2019): Upregulated expression of HOXB7 in intrahepatic cholangiocarcinoma is associated with tumour cell metastasis and poor prognosis. *Laboratory investigation; a journal of technical methods and pathology*, 99 (6): 736–748.
31. Zhou X, Liang T, Deng J *et al.* (2021): Differential and Prognostic Significance of HOXB7 in Gliomas. *Frontiers in cell and developmental biology*, 9: 697086. <https://doi.org/10.3389/fcell.2021.697086>
32. Zhang L, Wan Y, Zhang Z *et al.* (2021): IGF2BP1 overexpression stabilizes PEG10 mRNA in an m6A-dependent manner and promotes endometrial tumour progression. *Theranostics*, 11 (3): 1100–1114.
33. Wang J, Chen D, Zhang Y *et al.* (2023): Elevated expression of the RNA-binding protein IGF2BP1 enhances the mRNA stability of INHBA to promote the invasion and migration of esophageal squamous tumour cells. *Experimental hematology & oncology*, 12 (1): 75. <https://doi.org/10.7150/thno.49345>
34. Kim T, Havighurst T, Kim K *et al.* (2017): RNA-Binding Protein IGF2BP1 in Cutaneous Squamous Cell Carcinoma. *The Journal of investigative dermatology*, 137 (3): 772–775.
35. Lotfi E, Kholghi A, Golab F *et al.* (2024): Circulating miRNAs and lncRNAs serve as biomarkers for early colorectal tumour diagnosis. *Pathology-Research and Practice*, 255: 155187. <https://doi.org/10.1016/j.prp.2024.155187>